Iron Environment in Ferritin with Large Amounts of Phosphate, from *Azotobacter vinelandii* and Horse Spleen, Analyzed Using Extended X-ray Absorption Fine Structure (EXAFS)†

Jeffry S. Rohrer,‡ Quazi T. Islam,§ Gerald D. Watt,‖ Dale E. Sayers,§ and Elizabeth C. Theil*,‡

Departments of Biochemistry and Physics, North Carolina State University, Raleigh, North Carolina 27695, and Department of Chemistry, University of Colorado, Boulder, Colorado 80309

Received April 28, 1989; Revised Manuscript Received August 16, 1989

ABSTRACT: The iron core of proteins in the ferritin family displays structural variations that include phosphate content as well as the number and the degree of ordering of the iron atoms. Earlier studies had shown that ferritin iron cores naturally high in phosphate, e.g., *Azotobacter vinelandii* (AV) ferritin (Fe:P ratio = 1:1.7), had decreased long-range order. Here, the influence of phosphate on the local structure around iron in ferritin cores is reported, comparing the EXAFS of AV ferritin, reconstituted ferritin [the protein coats of horse spleen ferritin mixed with Fe(II) with and without phosphate at pH 7](Fe:P ratio = 1:0.25), and native horse spleen ferritin (Fe:P ratio = 1:0.125); reconstituted horse spleen ferritin without phosphate was indistinguishable from native horse spleen ferritin (HSF) in the analysis. In contrast, when the phosphate content was high in AV ferritin and horse spleen ferritin reconstituted with phosphate, the average iron atom had five to six phosphorus neighbors at 3.17 Å. Moreover, the number of detectable iron neighbors was lower when phosphate was high or present during reconstitution (2–3 vs 5–6), and the interatomic distance was longer (3.50 vs 3.03 Å), indicating that some phosphate bridges neighboring iron atoms. However, the decrease in the number of detectable iron–iron neighbors compared to HSF and the higher number of Fe–P interactions relative to Fe–Fe interactions suggest that some phosphate ligands were chain termini, or blocked crystal growth, and/or introduced defects which contributed both to the long-range disorder and to altered redox properties previously observed in AV ferritin.

Interactions of iron with phosphate have biological significance both molecularly and globally. On the one hand, variations occur in the phosphate content of ferritin from different sources, e.g., *Azotobacter vinelandii* (AV) vs horse spleen, and in different physiological conditions, e.g., normal and thalassemic human liver (Mann et al., 1986; Watt et al., 1986; Moore et al., 1986). On the other hand, volcanogenic activity under the ocean floor causes the release of particles of ferric oxide into the ocean which absorb phosphate (Berner, 1973). The consequent phosphate deficiency in the seawater limits the growth of plankton, which profoundly alters the ecology.

Ferritin iron cores can be crystalline (Harrison et al., 1967, 1987; Massower & Cowley, 1973), but in AV ferritin with a phosphate content 60% of the iron content (Mann et al., 1986; Watt et al., 1986) the iron core appears to be largely disordered as judged by electron microscopy (Mann et al., 1986) and Mössbauer spectroscopy (Watt et al., 1986). Phosphate also influences the magnetic interactions in the iron core of native and reconstituted ferritins (Williams et al., 1978). Although the physiological significance of the variations in the phosphate content of the iron core of the ferritins is not known, it is noteworthy that AV ferritin, which is relatively rich in phosphate, functions in the anaerobic environment of nitrogen fixation and has redox properties distinct from phosphate-poor ferritins (Watt et al., 1986).

In order to understand the effect of phosphate on the local structure of iron cores of ferritin, X-ray absorption spectra were collected and the EXAFS analyzed for AV ferritin (Fe:P ratio = 1:1.7), horse spleen ferritin (Fe:P ratio = 1:0.125), and ferritin reconstituted from the protein coats of horse spleen ferritin in the absence and presence of phosphate (Fe:P ratio = 1:0.25). The results, which show that phosphate reduces the number of near-iron neighbors (thus explaining the decrease in long-range order previously observed), are consistent with bridging phosphate, although some terminal phosphate is also likely.

Experimental Procedures

Horse spleen ferritin, twice crystallized and cadmium-free, was obtained from Boehringer Mannheim. AV ferritin was isolated as described earlier (Steifel & Watt, 1979). Protein coats were prepared by removing the iron by reduction and chelation as previously described (Chasteen & Theil, 1982); the iron content was <2–3/molecule. Reconstituted ferritin was prepared by mixing a solution of the protein coats in 0.15 M Hepes, pH 7, with a freshly prepared solution of $FeSO_4$ (480 Fe/molecule) for horse spleen ferritin reconstituted

† Beam line X-11 at the National Synchrotron Light Source (NSLS) is supported by the Division of Materials Science of the U.S. Department of Energy under Contract DE-AS05-80-Er 10742 (to D.E.S.). The NSLS is supported by the Division of Materials Science and the Division of Chemical Science of the U.S. Department of Energy under Contract DE-AC02-76CH00016. The Stanford Synchrotron Radiation Laboratory is supported by the Department of Energy Office of Basic Energy Services and the National Institutes of Health Biotechnology Research Programs, Division of Research Resources. Funds from the National Institutes of Health (GM34675) provided partial support for E.C.T. and J.S.R. This paper is a contribution from the Department of Biochemistry, College of Agriculture and Life Sciences and College of Physical and Mathematical Sciences, and from the Physics Department of the College of Physical and Mathematical Sciences. Paper 12156 of the Journal Series of the North Carolina Agricultural Research Service.

* Correspondence should be addressed to this author at the Department of Biochemistry, Box 7622, North Carolina State University, Raleigh, NC 27695-7622.

‡ Department of Biochemistry, North Carolina State University.

§ Department of Physics, North Carolina State University.

‖ Department of Chemistry, University of Colorado.

0006-2960/90/0429-259$02.50/0

Table I: Interactions of Fe with Nearest-Neighbors in Ferritin with and without Large Amounts of Phosphate from EXAFS Analysis[a]

sample	CN	r (Å)	$\Delta\sigma^2 \times 10^3$ (Å^2)	E (eV)	var $\times 10^5$
AV ferritin[b]	5.5 ± 0.5	1.95 ± 0.05	5.44 ± 0.5	3.50 ± 1	0.31
Fe:P = 1:1.7, HSFRECP[c]	5.0 ± 1	1.99 ± 0.04	6.00 ± 1	1.11 ± 0.4	4.8
Fe:P = 1:0.25, HSFREC[c]	5.0 ± 0.5	1.94 ± 0.04	7.40 ± 1	7.35 ± 0.5	6.5
Fe:P = 1:0, horse spleen ferritin, Fe:P = 1:0.125	5.0 ± 0.3	1.95 ± 0.01	4.2 ± 0.8	−1.4 ± 1.2	1.6

[a] The data presented were obtained from 2–3 independent samples measured at 2 different synchrotron laboratories and represent the results of 50 or more different fits for each sample; the analysis followed previous methods; see Islam (1989) and Experimental Procedures; the K weighting exponents used were 0–3, and the variance presented is for k weighting = 0. Data in the range 2–10 Å^{-1} were analyzed. The EXAFS range was 2–10 Å^{-1}, and the fitting range in the Fourier transform was 0.68–1.8 Å. [b] Ferritin isolated from *Azotobacter vinelandii* (Watt et al., 1986). [c] The protein coats of horse spleen ferritin (Fe = <2–3/molecule; see Experimental Procedures) reconstituted, in 0.15 M Na-Hepes, pH 7, with aqueous solutions of $FeSO_4$ to 480 Fe/molecule in the presence (HSFRECP) or absence of (HSFREC) $FePO_4 \cdot 7H_2O$.

without phosphate (HSFREC) with the addition of an aqueous solution of K_2HPO_4 at an Fe:P ratio = 1:0.25 for horse spleen ferritin reconstituted with phosphate (HSFRECP). Oxidation was allowed to proceed for at least 24 h before the X-ray absorption data were collected. Visual inspection of the samples showed that HSFRECP was green-brown, whereas HSFREC horse spleen ferritin and AV ferritin were reddish brown.

X-ray absorption data were collected on beam line II-1 at the Stanford Synchrotron Radiation Laboratory (SSRL) and on beam line X-11 at the National Synchrotron Light Source (NSLS) at room temperature in the fluorescence mode. The data were analyzed as previously described (Islam et al., 1989) using $Fe(NO_3)_3$ as a model for Fe–O (6 at 1.99 Å), $Fe^{II}O$ as a model for Fe–Fe (12 at 3.05 Å), and $FePO_4 \cdot 7H_2O$ as a model for Fe–P (4 at 3.33 Å). Note that Fe_2O_3 could be a better model for the Fe–Fe interaction except for the fact that the Fe–Fe shell is a mixture of three inseparable interactions; in contrast, Fe–O has only a single Fe–Fe interaction. The standards were measured as powders with the exception of $Fe(NO_3)_3$, which was measured in 0.1 M HNO_3 at a concentration of 50 mM, and the concentration of iron in each protein sample was 20 mM. Two independent samples of each type were prepared or purchased (horse spleen ferritin) and measured.

The definitions in Tables I–II are the following: CN, the coordination number; r, the interatomic distance; $\Delta\sigma^2$, the Debye–Waller factor relative to the standards; E, the shift of the energy origin of the data relative to that of the standard and the variance, a quantitative measure of the quality of the model. The uncertainties of all the parameters were determined by allowing some of the parameters to vary while constraining the others in such a way that the variance degraded to 50% of the best fit. The parameters obtained at these variances as well as the lowest variance were used with equal statistical weight to arrive at the results; the procedure ensures that the correlations among the parameters are accounted for in the errors. Visual inspection of the quality of fit was also used in selecting particular models. The models selected fit the best by visual inspection and also had at least a 10 times improvement quantitatively (compare, e.g., Figure 3a,b, Figure 4a,b, and Figure 3c,d).

Results

Nearest-Neighbor Iron–Oxygen/Nitrogen Interactions. Only one distance has been detected by EXAFS analysis among the nearest (O, N) neighbors of horse spleen ferritin with large iron cores at 1.95–1.99 Å (Islam et al., 1989; Yang et al., 1987). However, in a model dimeric iron complex, the inclusion of a phosphate bridge altered the length of an Fe–O bond (Armstrong & Lippard, 1985). The effect of phosphate on the interatomic distances of the nearest neighbors of iron in ferritin iron cores was analyzed by using EXAFS data (Figure 1) for AV ferritin (Fe:P ratio = 1:1.7), horse spleen

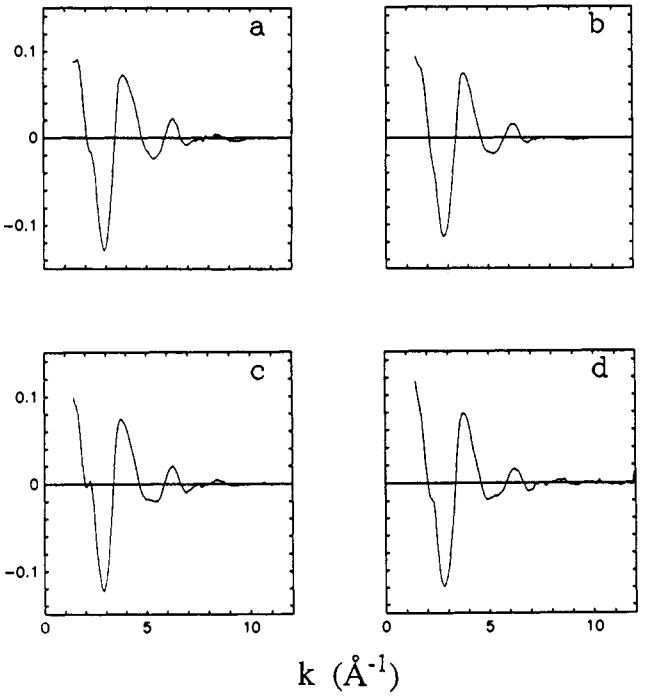

FIGURE 1: Normalized EXAFS of ferritin with various amounts of phosphorus. X-ray absorption spectra of solutions of ferritin samples varying in the amount of phosphorus were measured at room temperature in the fluorescence mode, and the data were analyzed as previously described (Islam et al, 1989; Yang et al., 1987; Mansour et al., 1985). (a) Ferritin from *Azotobacter vinelandii* (Fe:P ratio = 1.1.7); (b) the protein coat from horse spleen ferritin reconstituted to 480 Fe/molecule, 0.15 M Na-Hepes, pH 7 (see Experimental Procedures), in the presence of PO_4^- (Fe:P ratio = 1:0.25); (c) horse spleen ferritin (Fe:P ratio = 1:0.125); (d) ferritin protein coats reconstituted as in (b) in the absence of PO_4.

ferritin (Fe:P ratio = 1:0.125), and reconstituted horse spleen ferritin (480 Fe/molecule) with phosphate (HSFRECP, Fe:P ratio = 1:0.25) and without phosphate (HSFREC). Each data set was fit over the range (0.74–1.88 Å) of the Fourier transforms (Figure 2) with both one- and two-shell models. The two-shell model provided no improvement in the fits for any of the four samples, indicating that if there were two Fe–O/N distances when the phosphate content was high, the contribution of the second distance was too low to detect, either because it represents only a small fraction of the bonds or because it is disordered.

The results, presented in Table I, show that when phosphate was abundant in the native iron core (AV ferritin) or during reconstitution (HSFRECP), the near-neighbor environment was virtually indistinguishable from either native ferritin low in phosphate (horse spleen) or reconstituted ferritin (HSFREC); all the samples had 5–6 O/N neighbors at 1.94–1.99 Å. However, phosphate did change the optical properties of the iron core because HSFRECP was greenish brown compared to HSFREC or to horse spleen ferritin which

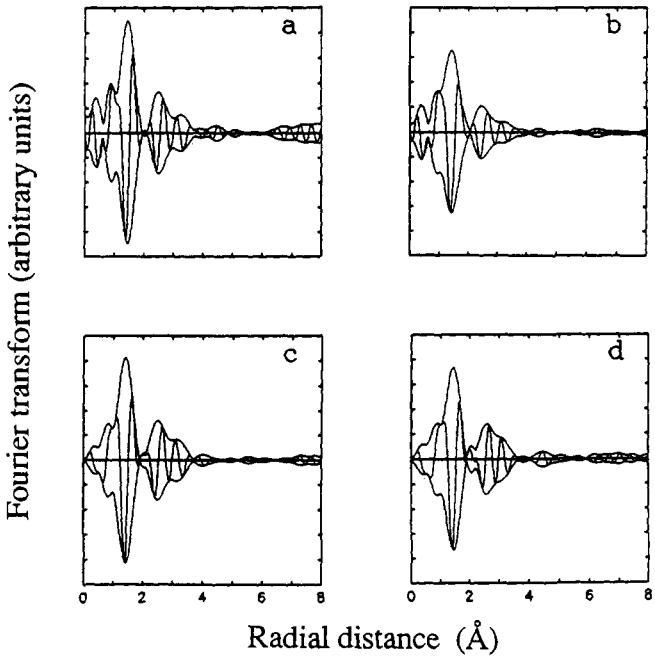

FIGURE 2: Fourier transform of EXAFS data for ferritin samples with varying amounts of phosphorus. Normalized EXAFS data in the range k = 2–10 Å^{-1} were transformed as previously described (Islam et al., 1989; Yang et al., 1987; Mansour et al., 1985); k = 3 weighting. (a) Ferritin from *Azotobacter vinelandii* (Fe:P ratio = 1.1.7). (b) The protein from horse spleen ferritin reconstituted to 480 Fe/molecule, 0.15 M Na-Hepes, pH 7 (see Experimental Procedures), in the presence of PO_4 (Fe:P ratio = 1:0.25). (c) Horse spleen ferritin (Fe:P ratio = 1:0.125). (d) Ferritin protein coats reconstituted as in (b) in the absence of PO_4.

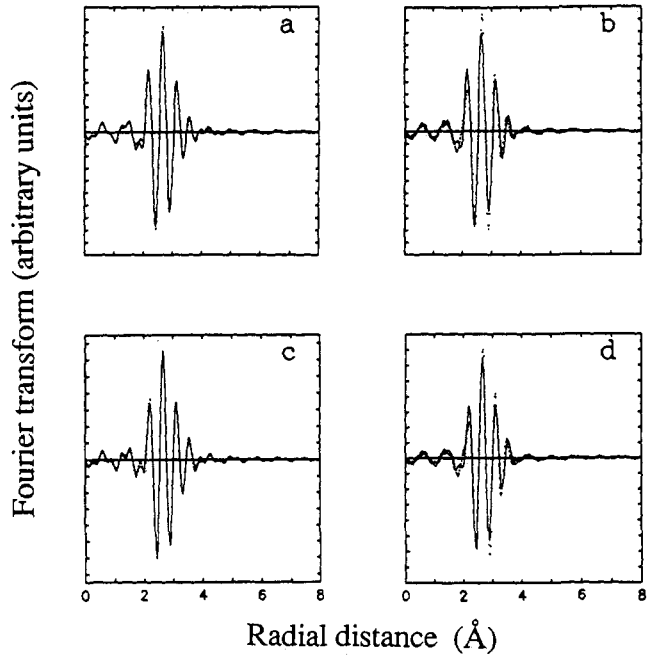

FIGURE 3: Comparison of the Fourier transform (imaginary) with the two-shell model of the iron–phosphorus and iron–iron interactions in horse spleen ferritin reconstituted with phosphate (Fe:P ratio = 1:0.25) and *Azotobacter vinelandii* ferritin. The data presented are for the range 2.02–3.50 Å (solid line) and various models (dotted line); when P–Fe are used in the models, the variance is so small, 2.4 × 10^{-7} or 2.1 × 10^{-8} for *Azotobacter vinelandii* ferritin and reconstituted ferritin, respectively, that the dotted line cannot be readily observed) (a, c); fitting the data over the ranges 2.02–2.78 and 2.78–3.50 Å gave comparable results. In contrast, when Fe–Fe are used and P omitted, the difference between the model data is readily observed (b, d). The Fe–P, Fe–Fe model fit the data qualitatively and quantitatively (10 times) better than the models with iron alone for AV ferritin and horse spleen ferritin reconstituted with phosphate, but the inclusion of phosphorus in the model of the data from horse spleen ferritin, native or reconstituted without phosphate, did not improve the fit.

were rust colored. AV ferritin contains heme and appeared reddish brown. (Note that the Fe–heme:Fe ratio in the core is only 0.013:1.00; heme–Fe would not be detectable at such a low relative concentration.)

Iron–Phosphorus and Iron–Iron Interactions. Properties of the P atom are sufficiently distinct from Fe or O/N to permit the detection of Fe–P interactions by EXAFS analysis of the data from binuclear iron complexes and from a complex of iron and ATP (Hedman et al., 1986; Kauzlarich et al., 1986; Mansour et al., 1985). For example, the difference in the back-scattering amplitude of Fe–P is large, and the phases differ; the back-scattering phase of Fe has a peak at 5 Å^{-1}, for example, whereas the corresponding function for P is monotonic.

Fe–P interactions in ferritins were analyzed by using the data from the Fourier transforms in the range of 2.02–3.50 Å. The data were fit with iron or phosphorus or oxygen as single models, or in many different combinations in two- or three-shell models. Final values for each parameter were arrived at by a series of successive approximations in which each parameter in turn was determined without restriction.

Visual inspection of the Fourier transforms shows the effect of phosphate. For example, the moduli of the transforms show significant differences between both HSFRECP and AV ferritin (Figure 2a,b) compared to both HSFREC and horse spleen ferritin (Figure 2c,d) in the region 2–4 Å. Of all the models tested, the two-shell model involving iron and phosphorus fit the data most closely (Figures 3–5). In addition, a quantitative measure of the difference between the data and the model (the variance) showed that the Fe–Fe and Fe–P models fit 10 times better than one-shell models or two-shell models with Fe–Fe, Fe–Fe or Fe–P, Fe–P. Three-shell models did not improve the fit to the data. EXAFS data from the fitting window used and the model are plotted together in

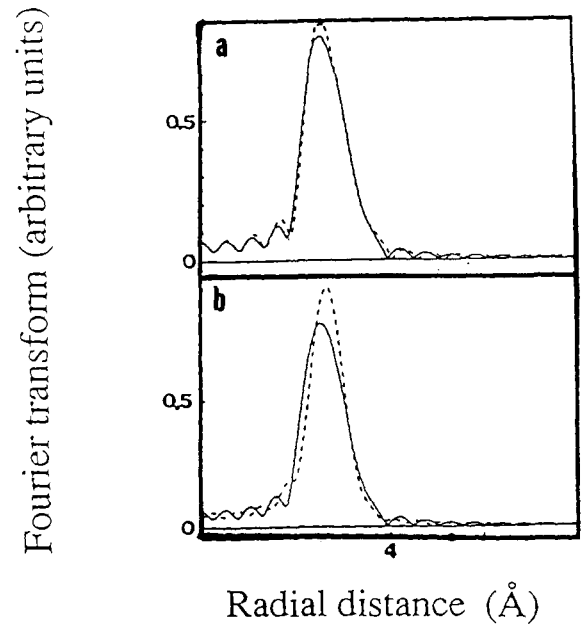

FIGURE 4: Comparison of the Fourier transform data with the two-shell model of iron–phosphorus and iron–iron interactions in horse spleen ferritin reconstituted with phosphate (Fe:P ratio = 1:0.25). The data presented are for the range 2.02–3.50 Å (solid line) and models (dotted line) after transformation of EXAFS data in the k space range 4–10 Å^{-1}. Note the improvement in the fit when both phosphorus and iron are included in the model (a) compared to Fe only (b); see also Figure 3.

Table II: Interactions of Iron with Phosphate and Iron Neighbors in Ferritin with and without Large Amounts of Phosphate from EXAFS Analysis[a]

sample	CN	r (Å)	$\Delta\sigma^2 \times 10^3$ (Å^2)	E (eV)	var $\times 10^6$
		Phosphate Neighbors			
AV ferritin[b] (Fe:P = 1:1.7)	5.0 ± 1	3.17 ± 0.04	−2.6 ± 0.1	3.7 ± 0.5	0.24
HSFRECP[c] (Fe:P = 4:1)	5.5 ± 0.5	3.17 ± 0.03	3.8 ± 0.4	3.9 ± 0.4	0.02
		Iron Neighbors			
AV ferritin[b] (Fe:P = 1:1.7)	1.6 ± 0.8	3.50 ± 0.02	0.79 ± 0.05	1.11	0.24
HSFRECP[c] (Fe:P = 4:1)	2.0 ± 0.4	3.50 ± 0.10	−2.6 ± 0.5	3.85 ± 0.4	0.021
HSFREC[c] (Fe:P = 1:0)	4.0 ± 0.5	3.03 ± 0.02	−0.88 ± 0.010	0.7 ± 0.2	5.4
	1.6 ± 0.2	3.51 ± 0.03	−0.55 ± 0.20	−6.0 ± 1.0	
horse spleen ferritin[d] (Fe:P = 1:0.125)	3.7 ± 0.4	3.00 ± 0.02	1.8 ± 1.8	4.5 ± 0.7	0.8
	2.0 ± 0.4	3.52 ± 0.03	−1.9 ± 2.4	4.8 ± 2.0	

[a] The data presented were obtained from 2–3 independent samples measured at 2 different synchrotron laboratories and represent the results of 50 or more different fits for each sample; the K weighting exponents used were 0–3; the variance is represented for K weighting = 0 to be consistent with Table I. EXAFS was analyzed in the k space range 4–10 Å^{-1}, and the fitting range of the Fourier transform used (Figure 2) was 2.04–3.50 Å; 2.02–2.78 and 2.78–3.50 Å were also used with the same results. The two-shell model phosphate with Fe, P, for samples with high phosphate, gave a 10-fold better fit than a single-shell model or a two-shell model with Fe–Fe and Fe–Fe (see, e.g., Figure 3a,c). Attempts to model the data by reversing the distances for Fe and P failed. [b] Ferritin isolated from *Azotobacter vinelandii* (Watt et al., 1986). [c] The protein coats of horse spleen ferritin (Fe = <2–3/molecule; see Experimental Procedures), reconstituted, in 0.15 M Na-Hepes, pH 7, with aqueous solutions of $FeSO_4$, to 480 Fe/molecule in the presence (HSFRECP) or absence of (HSFREC) $FePO_4 \cdot 7H_2O$. [d] Note that for horse spleen ferritin, native and reconstituted without phosphate, the two-shell model was 10 times better than a single-shell model. However, the neighbors at 3.5 Å were modeled equally well by Fe or O and at about 3.83 Å possibly because of greater disorder or back-scattering [see also Islam et al. (1989)].

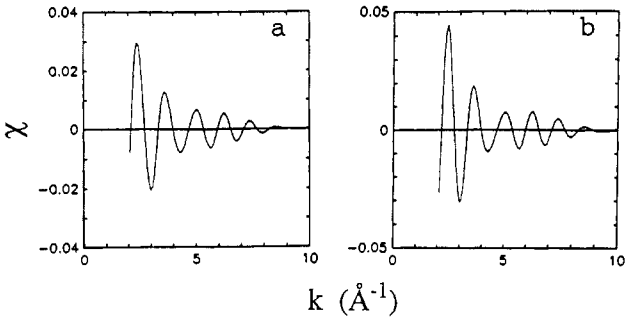

FIGURE 5: Comparison of EXAFS data with the two-shell model of iron–phosphorus interactions in horse spleen ferritin reconstituted with phosphate (Fe:P ratio = 1:0.25) and *Azotobacter vinelandii* ferritin. The data are presented for the range 2.0–3.5 Å (solid line) and the Fe–Fe, Fe–P model (dotted line). The fit is so close that the dotted line is essentially superimposed upon the solid line. (a) HSRECP; (b) AV ferritin.

Figure 5; Figures 3 and 4 are the Fourier transforms and the model. The variance is so small (10^{-7}) that the EXAFS data and model are essentially superimposable for AV ferritin and HSFRECP using the model containing both iron and phosphorus (Figure 5). The results of the two-shell (Fe, P) fit for neighbors in the transform range 2.04–3.50 Å show that when phosphate was present in large amounts (AV ferritin, Fe:P ratio = 1:1.7), or present during core formation (HSFRECP, Fe:P ratio = 1:0.25), an Fe–P interaction was detected at 3.17 Å (Table II); the average Fe atom had five to six P neighbors.

Fe–Fe interactions differed as well when P was high or present during core formation. For example, detectable Fe neighbors were only 2–3 in number and were at 3.5 Å (Table II) for AV ferritin or HSFREP; substituting P or O for Fe gave very poor fits, confirming the identity of the neighbor as Fe. However, when P was low as in horse spleen ferritin or HSFREC, five to six Fe neighbors were detected at 3.03 Å (Table II), confirming previous data (Islam et al., 1989). In addition, horse spleen ferritin and HSFREC also had two to three neighbors at ca. 3.5 Å which were fit equally well by Fe or O [see also Islam et al. (1989)]; thus, the identity of Fe as the more distant neighbor could not be established unequivocally for HSFREC in contrast to AV ferritin or HSREP. Substituting Fe for P at 3.17 Å and P for Fe at 3.50 Å produced an extremely poor fit, establishing that the neighbor at 3.17 Å was P and that the neighbors at 3.50 Å were not P. The difference in the results of EXAFS analysis of neighbors at 3.5 Å (Table II) in ferritins with high or low phosphate likely resides in a combination of factors that include back-scattering and molecular heterogeneity. At such long distances, similar ambiguities in other iron complexes including horse spleen ferritin have been observed as described in Islam et al. (1989) and Bunker et al. (1987), and appear to be structure dependent.

In order to evaluate the consistency of the modeled data, the more narrow ranges of 2.02–2.78 and 2.78–3.5 Å in the Fourier transform (Figure 2) were also tested with one- and two-shell models for the data for AV ferritin, horse spleen ferritin, HSFREC, and HSFRECP. The results were consistent with the Fe–Fe/Fe–P model for the longer range presented in Table II.

Discussion

The storage and controlled release of iron is a critical function of the ferritins because iron that is not specifically bound is toxic, insoluble, or both. For example, the versatility of iron in biological reactions such as photosynthesis, respiration, nitrogen fixation, and ribonucleotide reduction depends on the redox properties of iron which can also trigger potentially dangerous free radical reactions when iron is not bound or sequestered. Moreover, the acidic properties of hydrated ferric iron lead to the formation of large, oxo-bridged complexes which are insoluble. Ferritins can stabilize or sequester thousands of iron atoms as hydrous ferric oxides [reviewed in Harrison et al. (1987) and Theil (1987, 1989)] or as mixtures of ferrous and ferric species (Rohrer et al., 1987, 1989; Watt et al., 1985, 1986).

Variations occur in the structure of ferritin cores and/or the rates of reduction of ferritin iron (which precedes iron release in vitro at least) that depend upon the species or physiological state of the organism. Among the structural variables are iron core size, order or crystallinity, and phosphate content [e.g., see Mann et al. (1986, 1987), Mertz and Theil (1983), Moore et al. (1987), Treffry et al. (1987), and Weir et al. (1985)]. However, the specific effect of phosphate, e.g., on crystallinity/order and redox properties, is not clear, although it is known that phosphate also influences the crystallinity of magnetite (Couling & Mann, 1985) and that reconstitution of naturally phosphate rich AV ferritin in the absence of phosphate produces a core with increased long-

range order as judged by the detection of lattice images using high-resolution electron microscopy (Mann et al., 1987).

EXAFS analysis has permitted a comparison of the local environment around iron in ferritins varying in phosphate content either naturally (AV ferritin, Fe:P ratio = 1:1.7, vs horse spleen ferritin, Fe:P ratio = 1:0.125) or during reconstitution, using protein coats from horse spleen ferritin (HSFRECP, Fe:P ratio = 1:0.25, vs HSFREC, Fe:P ratio = 1:0). The results explain the observed decrease in the long-range order of ferritin iron cores when phosphate is high (Mann et al., 1986) and support an earlier prediction that phosphate can terminate the iron–oxo polymer (Theil, 1983).

The results showed that AV ferritin cores and reconstituted iron cores of horse spleen ferritin formed in vitro, from Fe(II), the protein coat, and phosphate, had local structures that were indistinguishable by EXAFS analysis, even though the total iron and phosphate contents differed (830 vs 480 iron atoms and 400 vs 120 P atoms for AV ferritin and reconstituted horse spleen protein, respectively). Both phosphate-rich ferritin iron cores had five to six oxygen (nitrogen) atoms at 1.95 Å as did native or reconstituted ferritin that was low in phosphate (Table I). However, the oxygen ligands appeared to include phosphate with five to six P neighbors at 3.17 Å in the phosphate-rich cores. No P could be detected by EXAFS analysis in the native or reconstituted iron core of horse spleen ferritin where phosphate was lower or absent; the inclusion of P in the models for native horse spleen ferritin or HSFREC did not improve the fit to the data whereas in the phosphate-rich ferritin iron cores, the inclusion of P in the model improved the quality of the fit very significantly. [The quantitative improvement was 10-fold (Figures 3–5).] Note that even though the Fe:P ratio in HSRECP was only 2 times higher than in native horse spleen ferritins, the effect was dramatic, suggesting that both stoichiometry and the presence of phosphate during core formation are important in the final core structure.

A comparison of the Fe–Fe interactions in phosphate-rich ferritin to low-phosphate ferritin showed that phosphate caused a lengthening of all iron–iron distances to 3.50 Å. A similar increase in the Fe–Fe distance was observed in a dimeric iron complex when a bridging carboxylate was replaced with a bridging phosphate (Armstrong & Lippard, 1985), suggesting that in AV ferritin, as well as in the reconstituted horse spleen ferritin with high phosphate, at least some of the phosphate groups bridge the iron neighbors. A second effect of phosphate on the iron–iron interaction is a reduction in the number of detectable iron neighbors, either because there is heterogeneity or because they are fewer in number or both. Moreover, the number of Fe–P neighbors in the phosphate-rich ferritin is higher (5–6) than the Fe neighbors (2–3) (Table II). Taken together, the results suggest that some of the phosphate ligands are nonbridging and represent termination sites in the iron–oxy polymer (crystallite). Such a conclusion was predicted previously (Theil, 1983) on the basis of earlier data (Granick & Hahn, 1944) and explains the reduced order (crystallinity) observed in AV ferritin (Mann et al., 1986).

The similarity of the local structure around the average iron atom in AV ferritin and in horse spleen ferritin reconstituted with phosphate (Fe:P ratio = 1:0.25) suggests that large amounts of phosphate can dominate over possible contributions of the protein coat to the structure of the core. A similar conclusion was reached from an X-ray diffraction study of AV ferritin and horse spleen ferritin reconstituted without phosphate (Mann et al., 1987). However, neither the EXAFS nor the X-ray diffraction experiments were designed to specifically examine protein–metal interactions, and thus it is premature to rule out the possible effects of the protein coat of ferritin on iron core nucleation in the presence and absence of phosphate.

Large amounts of phosphate clearly can influence the local structure, the long-range structure, and the redox properties of the ferritin iron core (Figures 1–5, Table II; Mann et al., 1986, 1987; Watt et al., 1986). However, whether the effect confers a biological advantage, enhancing the efficacy of iron storage in microorganisms such as *Azotobacter* and *Pseudomonas* (Mann et al., 1986; Moore et al., 1987; Watt et al., 1985), or whether the phosphate content of the ferritin iron core merely reflects environmental phosphate availability which must then be compensated for in vivo by changes in iron release, is not yet known. Whatever the case, the availability of ferritin iron cores of varying structures provides the opportunity to examine core formation and iron release with new perspectives.

Registry No. Fe, 7439-89-6; PO_4^{3-}, 14265-44-2.

References

Armstrong, W. H., & Lippard, S. J. (1985) *J. Am. Chem. Soc. 107*, 3730–3731.

Berner, R. A. (1973) *Earth Planet. Sci. Lett. 18*, 77–86.

Bunker, G., Peterson, L., Sjoberg, B. M., Sahlin, M., Chance, M., Chance, B., & Ehrenberg, A. (1987) *Biochemistry 26*, 4708–4716.

Chasteen, N. D., & Theil, E. C. (1982) *J. Biol. Chem. 257*, 7672–7677.

Couling, S., & Mann, S. (1985) *Chem. Commun.* 1713–1715.

Frankel, R. B., Papaefthymiou, G. C., Watt, G. D. (1987) *Hyperfine Interact. 33*, 233–240.

Granick, S., & Hahn, P. F. (1944) *J. Biol. Chem. 155*, 661–669.

Harrison, P. M., Fischbach, F. A., Hoy, T. G., & Haggis, G. H. (1967) *Nature 216*, 1188–1190.

Harrison, P. M., Andrews, S. C., Ford, G. C., Smith, J. M. A., Treffry, A., & White, J. L. (1987) in *Iron Transport in Microbes, Plants and Animals* (Winkelman, G., van der Helm, D., & Neilands, J. B., Eds.) pp 444–475, VCH, Weinheim and New York.

Hedman, B., Co, M. S., Armstrong, W. L., Hodgson, K. O., & Lippard, S. J. (1986) *Inorg. Chem. 25*, 2781.

Islam, Q. T., Sayers, D. E., Gorun, S. M., & Theil, E. C. (1989) *J. Inorg. Biochem. 36*, 51–62.

Kauzlarich, S. M., Teo, B. K., Zirino, T., Burman, S., Davis, J. C., & Averill, B. A. (1986) *Inorg. Chem. 25*, 2781–2785.

Mansour, A. N., Thompson, C., Theil, E. C., Chasteen, N. D., & Sayers, D. E. (1985) *J. Biol. Chem. 260*, 7975–7979.

Mann, S., Bannister, J. V., & Williams, R. J. P. (1986) *J. Mol. Biol. 188*, 225–232.

Mann, S., Williams, J., Treffry, A., & Harrison, P. M. (1987) *J. Mol. Biol. 198*, 405–416.

Massower, W. H., & Cowley, J. M. (1973) *Proc. Natl. Acad. Sci. U.S.A. 70*, 3847–3851.

Moore, G. R., Mann, S., & Bannister, J. V. (1986) *J. Inorg. Biochem. 28*, 329–336.

Rohrer, J. S., Joo, M. S., Dartyge, E., Sayers, D. E., Fontaine, A., & Theil, E. C. (1987) *J. Biol. Chem. 262*, 13385–13387.

Rohrer, J. S., Theil, E. C., Frankel, R. B., & Papaefythmiou, G. C. (1989) *Inorg. Chem. 28*, 3393–3395.

Steifel, E. I., & Watt, G. D. (1979) *Nature 279*, 81–83.

Theil, E. C. (1983) *Adv. Inorg. Biochem. 5*, 1–29.

Theil, E. C. (1987) *Annu. Rev. Biochem. 56*, 289–315.

Theil, E. C. (1989) *Adv. Enzymol. Relat. Areas Mol. Biol. 63*, 421–449.

Treffry, A., Harrison, P. M., Cleton, M. I., deBruijn, W. C., & Mann, S. (1987) *J. Inorg. Biochem.*, 1-6.
Watt, G. D., Frankel, R. B., & Papaefythymiou, G. C. (1985) *Proc. Natl. Acad. Sci. U.S.A. 82*, 3640-3643.
Watt, G. D., Frankel, R. B., Spartalian, K., & Steifel, E. I. (1986) *Biochemistry 25*, 4330-4336.
Weir, M. P., Gibson, J. F., & Peters, T. J. (1984) *Biochem. J. 223*, 31-38.
Williams, J. M., Danson, D. P., & Janot, C. H. R. (1978) *Phys. Med. Biol. 23*, 835-851.
Yang, C.-Y., Meagher, A., Huynh, B.-H., Sayers, D. E., & Theil, E. C. (1987) *Biochemistry 26*, 497-503.

Substrate Analogue Inhibition and Active Site Titration of Purified Recombinant HIV-1 Protease

Alfredo G. Tomasselli,[‡] Mary K. Olsen,[§] John O. Hui,[‡] Douglas J. Staples,[‡] Tomi K. Sawyer,[‡] Robert L. Heinrikson,*[,‡] and Che-Shen C. Tomich[§]

Biopolymer Chemistry and Molecular Biology Research Units, The Upjohn Company, Kalamazoo, Michigan 49001
Received June 21, 1989; Revised Manuscript Received August 9, 1989

ABSTRACT: The aspartyl protease of human immunodeficiency virus 1 (HIV-1) has been expressed in *Escherichia coli* at high levels, resulting in the formation of inclusion bodies which contain denatured insoluble aggregates of the protease. After solubilization of these inclusion bodies in guanidinium chloride, the protease was purified to apparent homogeneity by a single-step reverse-phase HPLC procedure. The purified, but inactive, protein was denatured in 8 M urea and refolded to produce the active protease. Enzyme activity was demonstrated against the substrate H-Val-Ser-Gln-Asn-Tyr-Pro-Ile-Val-OH, modeled after the cleavage region between residues 128 and 135 in the HIV gag polyprotein. With this substrate, a V_{max} of 1.3 ± 0.2 μmol/(min·mg) and K_M of 2.0 ± 0.3 mM were determined at pH 5.5. Pepstatin (Iva-Val-Val-Sta-Ala-Sta-OH) and substrate analogues with the Tyr-Pro residues substituted by Sta, by PheΨ[CH_2N]Pro, and by LeuΨ[CH(OH)CH_2]Val inhibited the protease with K_I values of 360 nM, 3690 nM, 3520 nM, and <10 nM, respectively. All were competitive inhibitors, and the tightest binding compound provided an active site titrant for the quantitative determination of enzymatically active HIV-1 protease.

Human immunodeficiency virus (HIV), a member of the retrovirus group, has been recognized as the causative agent of acquired immunodeficiency syndrome (AIDS) (Weiss et al., 1985; Gallo & Montagnier, 1988). The molecular organization of the HIV genome comprises *gag*, *pol*, and *env* as genes necessary for viral replication (Dickson et al., 1984; Ratner et al., 1985). During viral replication, these genes are expressed as polyproteins which undergo enzymatic cleavage to generate the functional proteins of the mature virus. Genetic and biochemical studies have demonstrated that a virally encoded protease is responsible for the release of protease (autoproteolysis), reverse transcriptase, integrase, and other proteins from the *gag-pol* fusion proteins (Crawford & Goff, 1985; Katoh et al., 1985; Darke et al., 1988; Krausslich & Wimmer, 1988; Le Grice et al., 1988). Recently, the HIV-1 protease has been proven to be essential for viral maturation; site-directed mutagenesis of the protease active site leads to the loss of viral infectivity (Kohl et al., 1988).

The HIV-1 protease consists of only 99 amino acids, and its demonstrated activity and homology to aspartyl proteases such as pepsin and renin (Katoh et al., 1987; Seelmeier et al., 1988; Loeb et al., 1989) led to inferences regarding the three-dimensional structure and mechanism of the enzyme that have since been borne out experimentally (Pearl & Taylor, 1987; McKeever et al., 1989; Miller et al., 1989; Navia et al., 1989; Weber et al., 1989). To obtain quantities of HIV-1 protease needed for biophysical and structural characterization and for testing of inhibitors, a number of laboratories have produced the enzyme either by chemical synthesis (Copeland & Oroszlan, 1988; Nutt et al., 1988; Schneider & Kent, 1988) or by expression in *Escherichia coli* (Farmerie et al., 1987; Debouck et al., 1987; Giam & Boros, 1988; Graves et al., 1988; Hansen et al., 1988; Mous et al., 1988; Darke et al., 1989; Krausslich et al., 1989; Meek et al., 1989). Some of these preparations have been used to test synthetic peptides as substrates and inhibitors (Billich et al., 1988; Darke et al., 1988; Kotler et al., 1988; Moore et al., 1989; Meek et al., 1989; Richards et al., 1989).

Here we report the high-level expression of the HIV-1 protease in *E. coli*; accumulation of the enzyme results in its deposition as insoluble aggregates. A rapid HPLC purification of the protease from these solubilized inclusion bodies, followed by a denaturation/refolding step, yields a homogeneous preparation of active enzyme. This enzyme has been characterized structurally and kinetically, and inhibition constants have been determined with pepstatin and several substrate-based derivatives as inhibitors of the protease. One tight-binding substrate analogue provided titration of the functional catalytic sites in our purified recombinant protease preparation.

Materials and Methods

Enzymes, Oligonucleotides, and Plasmid Constructions. Restriction endonucleases, T4 DNA ligase, and T4 poly-

[‡] Biopolymer Chemistry Research Unit.
[§] Molecular Biology Research Unit.

0006-2960/90/0429-264$02.50/0